

Modification of Selection Rules of Landau-Quantized Electron by Coupling with Obliquely Irradiated Optical Vortex Beams

Hirohisa T. Takahashi

*Academic Support Center, Kogakuin University of Technology & Engineering,
2665-1 Nakano, Hachioji, Tokyo 192-0015, Japan**

Jun-ichiro Kishine

*Division of Natural and Environmental Sciences,
The Open University of Japan, Chiba 261-8586, Japan and
Institute for Molecular Science, 38 Nishigo-Naka,
Myodaiji, Okazaki 444-8585, Japan*

(Date textdate)

Abstract

We discuss selection rules and intensities of photocurrent of a two-dimensional electron gas in a strong magnetic field via absorptions of orbital angular momentum carried by obliquely irradiated optical vortex beams. By angular deflection, optical vortex beams on the two-dimensional electron gas interface can be seen as a superposition of the various orbital angular momentum states. As a result, it is demonstrated that it is yielded that the angular momentum selection rules and induced currents are modified from the case of vertical incidence.

PACS numbers: 42.50.Tx, 71.70.Di, 78.20.Ci

I. INTRODUCTION

It is theoretically pointed out that lights with a circular polarization can exert torque by Poynting in 1909,[1] and it is experimentally demonstrated that circularly-polarized lights carry angular momentum of $\pm\hbar$, namely, spin angular momentum (SAM) by Beth in 1936.[2] In 1992, an optical vortex beam (OV beam) was proposed by L. Allen *et al.*. They pointed out that light beams can also carry an intrinsic orbital angular momentum (OAM).[3] OV carries an OAM $\ell\hbar$ by an azimuthal phase dependence of $e^{i\ell\phi}$ with an integer ℓ . The integer ℓ is the winding number of the helical wavefront. The azimuthal phase dependence makes ℓ intertwined helical wavefront. Hereafter, we refer to the winding number ℓ as an orbital number. Then, it is known that OV with non-zero OAM has a phase singularity on its optical axis. A Laguerre-Gaussian mode (LG-mode) is well known as one of the radial intensity modes. Several ways to product the LG-mode OV are known: directly productions,[4, 5] conversion from Hermite-Gaussian modes,[3, 6] the use of spiral phase plates,[7] the use of computer-generated holograms,[8] diffractive optics,[9] or semiconductor microcavity.[10] The LG-mode beam has the nature of gradually expanding the beam as it propagates.

Besides the LG-mode, Bessel-mode OV is also well known as the radial function mode.[11] In general, the amplitude of Bessel-mode OV in cylindrical coordinates (r, ϕ, z) can be described by

$$E(r, \phi, z) \propto J_\ell(k_\perp r) e^{ik_z z} e^{i\ell\phi}, \quad (1)$$

* kt13673@ns.kogakuin.ac.jp

where $J_\ell(x)$ is an ℓ -th order Bessel function of the first kind, k_z and k_\perp are respectively the longitudinal and transverse wavenumber satisfying $k = \sqrt{k_z^2 + k_\perp^2}$. It thus has a cylindrical intensity distribution consisting of bright and dark rings. In particular, since its intensity ($I \propto |E|^2$), obeys $I(r, \phi, z \geq 0) = I(r, \phi)$, the intensity is invariant under the propagation of the beam. That is to say, the Bessel-mode beam can be considered diffraction-free.[12, 13] The Bessel-mode OV can be created, in the back focal plane of a convergent lens by a plane wave,[14] or in that of an axicon from a Gaussian beam.[15] Besides, it can be created by the use of computer-generated holograms,[16] or by a Fabry-Perot resonator.[17]

The transfer of optical OAM to physical matters has much got attracted and actively been researched. For examples, the transfer to classical particles as an optical tweezer,[18, 19] to exciton center-of-mass motion,[20] to the bounded electron in atoms,[21] or the laser ablation technique[22] have been demonstrated. Various theoretical predictions in condensed matter physics have also done: the optical absorption by semiconductors,[23] an electric current density in a semiconducting stripe,[24] the excitation of multipole plasmons in metal nanodisks,[25], the spin and charge transport on surface of topological insulators,[26], the generation of skyrmionic defects in chiral magnets,[27] and the creation of superconducting vortices,[28] among other things.

However, it is known that an exchange of the optical OAM does not occur in an electric dipole transition in atoms and molecules.[29] It is still an open question how optical OAM affects electronic transitions. To fully exchange the optical OAM to the electron center-of-mass motion in electric dipole transitions, it is needed the conformity of the electron distribution with the OV intensity distribution. Therefore, in our previous paper,[30] we considered two-dimensional electron gas (2DEG) as one of the good candidates. It is because an axial symmetric 2DEG has the cylindrical electron distribution as the coherent state. Thus our previous work was focused on the case of vertical incidence of OV beams. As a result, we obtained the selection rules in the electric dipole transitions from the lowest Landau level (LLL) to the second Landau level (2LL) as

$$\ell = 2, \sigma = -1, \text{ and } \ell = 0, \sigma = 1 \tag{2}$$

with optical spin number σ . However, from experimental viewpoints, it is quite natural to consider the case of oblique incidence. In the case of oblique incidence, the incident beam carries a definite OAM, but the irradiated beam consists of a superposition of various OAM

states.[31, 32] Therefore, it is expected that the AM selection rules and behaviors of OV-induced photocurrents are modified. In this paper, we investigate the modification of the selection rules from Eq. (2) and numerically demonstrate the incident angle and magnetic field dependence of OV-induced photocurrents by the oblique irradiation (angular deflection) of OV beams to the reference axis of 2DEG.

This paper is organized as follows. In Section II, we describe a circularly-polarized Bessel-mode optical vortex (CPBOV) beam in oblique irradiation. We calculate the induced photocurrent in 2DEG by obliquely irradiated CPBOV in Sec. III. In Sec. IV, we show numerical results of the incident angle and magnetic field dependence of the OV-induced photocurrent. Sec. V is reserved for conclusions and remarks.

II. DESCRIPTION OF OBLIQUELY INCIDENT OPTICAL VORTEX BEAM

It is crucial for studying the properties of light to separate a total angular momentum (TAM) into a spin and orbital AM since they are then separately conserved when interacting with particles. In electromagnetism, the TAM density of the electromagnetic field is generally given by the vector product of the radial vector and the linear momentum density. But such a form is typically similar to the form for an orbital angular momentum for a rigid body in mechanics. This curious fact shows the difficulties in separating the TAM into the spin and orbital parts for an electromagnetic field. In a paraxial approximation, such the light beam has a well-defined separation of the TAM into the spin and orbital AMs. Then it becomes natural to define optical OAM to its optical axis and optical OAM is identified as the eigenvalue of the quantum mechanical AM operator.[33] Therefore, a discrete OAM spectrum (orbital number) is produced. This is the result of an axially symmetric structure of the light beam.

Generally, the optical OAM depends on the choice of the reference axis of the system.[34, 35] If the axial symmetric structure is broken, *e.g.* by a lateral displacement or angular tilt of the beam, the reference axis is changed and it is impossible to determine the reference axis for a nonsymmetric beam. In particular, the initially carrying OAM transforms to the superposition of OAM states in a changed coordinate frame. Nevertheless, such the transformed beam with a well-defined OAM can be described in the form of an infinite set of azimuthal harmonics in the form of Bessel functions.[31] Therefore, it is allowed the

evaluation of the interaction of the nonsymmetric beam with microscopic particles in a quantitative way. In this paper, to investigate contributions of an OAM of light to 2DEG via AM selection rules, we adopt an OV beam in a paraxial approximation, in particular, a circularly polarized Bessel-mode optical vortex beam (CPBOV beam). We then concentrate on the case of the angular deflection to the reference axis and describe its vector potential of CPBOV in this section.

We assume the vector potential of OV is taken in the form of the monochromatic beam, $\mathbf{A}^{\text{OV}}(\mathbf{r}, t) = \mathbf{A}^{\text{OV}}(\mathbf{r}) e^{-i\omega t}$. By introducing the longitudinal wavenumber along to the beam axis k_{\parallel} and its transverse wavenumber k_{\perp} , the spatial part of the vector potential of CPBOV traveling along Z -direction in the beam frame is given by[11, 36]

$$\mathbf{A}_{\ell,\sigma}^{\text{OV}}(\mathbf{r}|\theta) = \varepsilon_{\sigma} A_0 \sqrt{\frac{k_{\perp}}{2\pi}} i J_{\ell}(k_{\perp} R_{\perp}) e^{i\ell\Phi} e^{ik_{\parallel}Z}, \quad (3)$$

where A_0 is a real constant, ℓ is a topological number of OAM, and $J_{\ell}(x)$ is ℓ -th order Bessel function of the first kind. Because of $J_{\ell}(k_{\perp} R_{\perp})$, the beam profile has cylindrical intensity distribution. The superscript 'BF' indicates the quantity in the beam frame. $k = \omega/c = \sqrt{k_{\perp}^2 + k_{\parallel}^2}$ is the magnitude of wavenumber with the speed of light in vacuum c , and the frequency ω . By introducing a ratio $\alpha = k_{\perp}/k_z (\ll 1)$, the transverse wavenumber is given by $k_{\perp} = \sqrt{k^2 - k_{\parallel}^2} \sim \alpha k$. The polarization vectors in the beam frame are taken on the helicity basis,

$$\varepsilon_{\sigma} = \frac{1}{\sqrt{2}} (\mathbf{e}_X + i\sigma\mathbf{e}_Y), \text{ for } \sigma = \pm 1, \quad (4)$$

which gives $\hat{S}_Z \mathbf{A}_{\ell,\sigma}^{\text{OV}}(\mathbf{r}) = \hbar\sigma \mathbf{A}_{\ell,\sigma}^{\text{OV}}(\mathbf{r})$. Here \hat{S}_Z is the Z -component of the SAM operator. The Z -component of the OAM operator is

$$\hat{L}_Z = -i\hbar \frac{\partial}{\partial \Phi}, \quad (5)$$

which gives

$$\hat{L}_Z \mathbf{A}_{\ell,\sigma}^{\text{OV}}(\mathbf{r}) = \hbar\ell \mathbf{A}_{\ell,\sigma}^{\text{OV}}(\mathbf{r}). \quad (6)$$

Then, the Z -component of the TAM of the beam, $\hat{J}_Z = \hat{L}_Z + \hat{S}_Z$, is given by $J = \ell + \sigma$.

To discuss the oblique irradiation of OVs to a 2D system after this, since the expression (3) is described in the beam frame, we need to describe the vector potential on the 2D plane (the Laboratory frame). We then describe the beam frame by the Cartesian coordinate as (X, y, Z) , where the light beam is traveling along Z -axis. R_{\perp} and Φ are the radial component

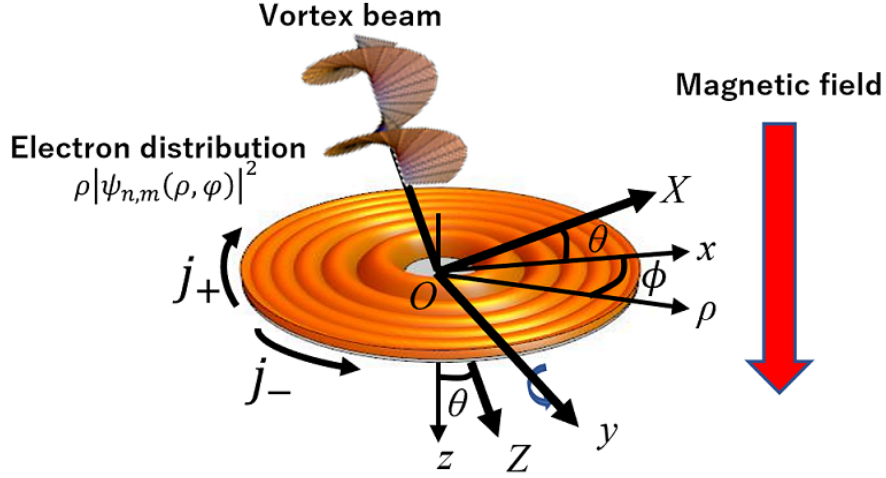


FIG. 1. The setup configuration. The laboratory frame (x, y, z) is chosen the xy -plane being on the 2DEG plane and the z -axis being on the normal to the plane. The z -axis is then the reference axis. The azimuthal angle ϕ of the cylindrical coordinates on the laboratory frame is measured from the x -axis. The beam frame (X, y, Z) is chosen as the Z -axis to the beam axis and the Xy -plane is rotated xy -one around the y -axis with angle θ .

and azimuthal angle on Xy -plane, respectively. We here refer to the rotation around the y -axis by the angle θ from the laboratory frame (x, y, z) to the beam frame (X, y, Z) as shown in Fig.1. Thus we can consider the beam traveling at an incident angle θ to the reference axis z . The unit vectors \mathbf{e}_i are then transformed by the rotation matrix $\mathcal{R}_y(\theta)$ as

$$\begin{pmatrix} \mathbf{e}_X \\ \mathbf{e}_y \\ \mathbf{e}_Z \end{pmatrix} = \mathcal{R}_y^{-1}(\theta) \begin{pmatrix} \mathbf{e}_x \\ \mathbf{e}_y \\ \mathbf{e}_z \end{pmatrix} \quad \text{with} \quad \mathcal{R}_y(\theta) = \begin{pmatrix} \cos \theta & 0 & -\sin \theta \\ 0 & 1 & 0 \\ \sin \theta & 0 & \cos \theta \end{pmatrix}. \quad (7)$$

First, we discuss the transformation of the polarization. By the transformation (7), the polarization in the Laboratory frame η_σ is given by

$$\begin{aligned} \eta_\sigma &= \mathcal{R}_y(\theta) \varepsilon_\sigma \\ &= \frac{1}{\sqrt{2}} (\cos \theta \mathbf{e}_x + i\sigma \mathbf{e}_y - \sin \theta \mathbf{e}_z). \end{aligned} \quad (8)$$

Thus, in the laboratory frame, the polarization of the obliquely-irradiated beam with circular polarization behaves as the elliptic polarization with ellipticity, $\tan \chi = 1/\cos \theta$. Also, the

circular shape of the profile of CPBOV changes into an elliptic shape. Because the argument of $J_\ell(k_\perp R_\perp)$ in the Laboratory frame is written by

$$k_\perp R_\perp = k_\perp \rho [\cos^2 \theta \cos^2 \phi + \sin^2 \phi]^{\frac{1}{2}}, \quad (9)$$

where we introduced the cylindrical coordinates in the laboratory frame as (ρ, ϕ, z) as shown in Fig.1. Furthermore, to fully describe the vector potential of obliquely irradiated OV in Laboratory frame, we also need the transformation of the azimuthal phase factor $e^{i\ell\Phi}$ and the traveling wave sector $e^{ik_\parallel Z}$. The azimuthal phase factor $e^{i\ell\Phi}$ are rewritten as

$$\begin{aligned} e^{i\ell\Phi} &= e^{i\ell \arctan\left(\frac{\tan \phi}{\cos \theta}\right)} \\ &= \frac{(\cos \theta \cos \phi + i \sin \phi)^\ell}{(\cos^2 \theta \cos^2 \phi + \sin^2 \phi)^{\frac{\ell}{2}}}. \end{aligned} \quad (10)$$

And the traveling wave sector $e^{ik_\parallel Z}$ can be expanded as

$$e^{ik_\parallel Z} = e^{ik_\parallel z \cos \theta} \sum_{L=-\infty}^{\infty} e^{iL\frac{\pi}{2}} J_L(k_\parallel \rho \sin \theta) e^{iL\phi}, \quad (11)$$

by the Jacobi-Anger expansion (the partial wave expansion) and the Bessel function of the first kind with L in an integer.[37] When we restrict our discussion to the region that the incident angle θ is sufficiently small. Then, it satisfies $\sin \theta \sim \theta$ and $\cos \theta \sim 1$. Thus the vector potential in the laboratory frame arrives at

$$\begin{aligned} \mathbf{A}_{\ell,\sigma}^{\text{OV}}(\mathbf{r}|\theta) &\sim (\mathbf{e}_x + i\sigma\mathbf{e}_y - \theta\mathbf{e}_z) A_0 \sqrt{\frac{k_\perp}{4\pi}} J_\ell(k_\perp \rho) \\ &\times e^{ik_\parallel z} \sum_{L=-\infty}^{\infty} J_L(k_\parallel \rho \theta) e^{i(\ell+L)\phi} e^{i(L+1)\frac{\pi}{2}}. \end{aligned} \quad (12)$$

It appears the changes of the azimuthal phase factor as $\exp[i(\ell+L)\phi]$ and of the radial profile function as $J_\ell(k_\perp \rho) J_L(k_\parallel \rho \theta)$. This physical meaning is that CPBOVs can be seen as a superposition of waves with OAM, $\ell+L$. [31, 38]

As mentioned in detail later, the partial wave expansion (12) plays an important role and gives birth to curious results. As the CPBOVs are constituted by the superposition of the OAM $\ell+L$ state, they modify the optical AM selection rules. Also, the factor $J_L(k_\parallel \rho \theta)$ also contributes to the oscillatory behavior of the OV-induced photocurrent in the change of incident angle θ .

III. PHOTOCURRENT INDUCED BY OBLIQUELY IRRADIATED OPTICAL VORTEX BEAM

Landau-quantized energy spectrum appears when a strong magnetic field is uniformly applied to a 2-dimensional electron gas (2DEG) perpendicular to the specimen surface. The energy spectrum of the standard Landau-quantized state, $E_N = \hbar\omega_c(N + 1/2)$, appears under a Landau gauge (suitable for a rectangle specimen), where N is a positive integer, $\omega_c = eB/m_e$ is the cyclotron frequency with the elementary charge $e (> 0)$, the strength of the magnetic field B , and the electron mass m_e . For a circular disk geometrical specimen, the energy spectrum explicitly depends on an OAM of the electron under the symmetric gauge. This is a manifestation that the symmetric gauge preserves axial symmetry. Thus an electron OAM becomes a good quantum number. For these reasons, a circular disk geometrical specimen is the best choice to observe the induced current by the interaction with lights carrying an OAM.

The Hamiltonian for 2DEG applying the perpendicular magnetic field in the z -axis direction is given by

$$H_0 = \frac{1}{2m_e} [-i\hbar\nabla + e\mathbf{A}^{\text{ext}}(\mathbf{r})]^2, \quad (13)$$

with symmetric gauge, $\mathbf{A}^{\text{ext}}(\mathbf{r}) = (-By/2, Bx/2, 0)$. Then the energy spectrum and the wavefunction in cylindrical coordinates (ρ, ϕ, z) in the laboratory frame are respectively written as

$$\begin{aligned} E_{n,m} &= \hbar\omega_c \left(N + \frac{1}{2} \right) \\ N &= n + \frac{|m| + m}{2}, \\ n &= 0, 1, 2, \dots, \text{ and } m = 0, \pm 1, \pm 2, \dots, \end{aligned} \quad (14)$$

and,

$$\begin{aligned} \Psi_{nm}(\rho, \phi) &= N_{nm} e^{-\frac{\rho^2}{4l_B^2}} \left(\frac{\rho}{l_B} \right)^{|m|} L_n^{|m|} \left(\frac{\rho^2}{2l_B^2} \right) \frac{e^{im\phi}}{\sqrt{2\pi}} \\ &\equiv \mathfrak{R}_{n,m}(\rho) \frac{e^{im\phi}}{\sqrt{2\pi}}, \end{aligned} \quad (15)$$

where n is a principal quantum number and m , an electron orbital number.[39] Here we denoted the normalization constant is $N_{nm} = [n!/(n + |m|)!]^{\frac{1}{2}} 2^{-|m|/2} l_B^{-1}$, $L_n^{|m|}(x)$ is the as-

sociated Laguerre polynomials, and $l_B = \sqrt{\hbar/eB}$ is the magnetic length. The boundary condition gives the degeneracy factor of each Landau level, $m_{\max} = R^2/2l_B^2$, where R is the fixed radius of the circular disk geometry (the system size). The filling factor is defined as $\nu = N_e/m_{\max}$, where N_e is the total number of electrons.

In this section, we provide the quantitative analysis of the induced photocurrent via the transfer of optical AM. To see this, we investigate the interaction between a Landau-quantized 2DEG and CPBOV at the $z = 0$ plane. We start with the total Hamiltonian, which is configured by the 2DEG Hamiltonian (13) and light-electron coupling one, $H_{\text{int}} = -\mathbf{A}_{\ell,\sigma}^{\text{OV}}(\theta) \cdot \mathbf{j}$:

$$H = H_0 + H_{\text{int}} = \frac{1}{2m_e^*} [-i\hbar\nabla + e\mathbf{A}^{\text{ext}}(\mathbf{r})]^2 - \mathbf{A}_{\ell,\sigma}^{\text{OV}}(\theta) \cdot \mathbf{j}, \quad (16)$$

where $\mathbf{A}_{\ell,\sigma}^{\text{OV}}(\theta)$ is the spatial part of CPBOV vector potential which travels along the Z -axis (12), and the photocurrent operator is given by $\mathbf{j} = e(\mathbf{p} + e\mathbf{A}^{\text{ext}})/m_e$. By an extremely strong magnetic field, the spin degree of freedom is frozen, and we can neglect the degree of spin of an electron.

To see the induced photocurrent, we apply the linear response theory. This is justified when the electric and magnetic fields of OV are sufficiently weak. Thus we start with the Kubo formula for i component of the response current[40, 41] :

$$\begin{aligned} \delta j_i(\omega) &= -\frac{1}{V} \sum_{n,m} \sum_{n',m'} (f(E_{n,m}) - f(E_{n',m'})) \\ &\times \frac{\langle n, m | j_i | n', m' \rangle \langle n', m' | \mathbf{A}_{\ell,\sigma}^{\text{OV}}(\theta) \cdot \mathbf{j} | n, m \rangle}{E_{n,m} - E_{n',m'} + \hbar\omega + i\delta}. \end{aligned} \quad (17)$$

where V is the volume of the system and $f(E_{n,m})$ is the Fermi distribution, $f(\epsilon) = [\exp \beta(\epsilon - \mu) + 1]^{-1}$ with the chemical potential μ and the inverse temperature β . We note that we do not take account of any impurity effects in this paper. Although the impurity-induced relaxation may provide the imaginary part of the electron self-energy, τ^{-1} , in a real system, we added a positive infinitesimal δ in the denominator to give the numerical analysis below. We concentrate on zero temperature, $T = 0$.

The matrix element of the photocurrent operator in a chiral basis, $j_{\pm} = (j_x \mp ij_y)/\sqrt{2}$, where the upper (under) sign corresponds to the right (left)-circularly polarized photocurrent is written as

$$\langle n, m | j_{\pm} | n', m' \rangle = i \frac{e}{\sqrt{2}\hbar} (E_{n,m} - E_{n',m'}) C_{n,m}^{n',m'} \delta_{\Delta m, \pm 1} \quad (18)$$

where we denoted $\Delta m = m' - m$, and the radial integral as

$$C_{n,m}^{m',m'} = \int d\rho \rho^2 \mathfrak{R}_{n',m'}(\rho) \mathfrak{R}_{n,m}(\rho). \quad (19)$$

From the azimuthal integral, we obtain the selection rule,

$$\Delta m = \pm 1, \quad (20)$$

The $+$ ($-$) in (20) corresponds to the result of the right (left)-circularly polarized current, respectively. Further by performing the radial integral and calculating the energy factor, $E_{n,m} - E_{n',m'}$ with Eq.(14), we also obtain the matrix elements for the photocurrent operator matrix as

$$\langle n, m | j_+ | n', m + 1 \rangle = \begin{cases} -iel_B \omega_c \sqrt{n + \frac{|m|+m}{2} + 1}, & \text{for } n' = n \text{ and } m \geq 0, \\ iel_B \omega_c \sqrt{n + \frac{|m|+m}{2} + 1}, & \text{for } n' = n + 1 \text{ and } m \leq -1, \\ 0, & \text{for otherwise,} \end{cases} \quad (21)$$

$$\langle n, m | j_- | n', m - 1 \rangle = \begin{cases} iel_B \omega_c \sqrt{n + \frac{|m|+m}{2}}, & \text{for } n' = n \text{ and } m \geq 1, \\ -iel_B \omega_c \sqrt{n + \frac{|m|+m}{2}}, & \text{for } n' = n - 1 \text{ and } m \leq 0, \\ 0, & \text{for otherwise.} \end{cases} \quad (22)$$

Then, if the LLL, $N = 0$, is filled by electrons (which corresponds to the filling factor being set to $\nu = 1$), the Pauli exclusion principle allows for the transitions from the LLL to the 2LL, $N = 1$. Consequently, the element, $\langle n, m | j_+ | n', m' \rangle$ survives only for

$$\Delta m = 1. \quad (23)$$

and the possible transitions are limited to the cases,

$$\begin{aligned} (n, m, N) & \quad (n', m', N') \\ (0, 0, 0) & \rightarrow (0, 1, 1), \quad \text{for } m = 0, \\ (0, m, 0) & \rightarrow (1, m + 1, 1), \quad \text{for } m < 0. \end{aligned} \quad (24)$$

Next, to calculate the matrix element of the light-electron coupling, $\langle n', m' | \mathbf{A}_{\ell,\sigma}^{\text{OV}}(\theta) \cdot \mathbf{j} | n, m \rangle$, we apply the long-wavelength approximation. Then the matrix element reduces to

$$\begin{aligned} & \langle n', m' | \mathbf{A}_{\ell,\sigma}^{\text{OV}}(\theta) \cdot \mathbf{j} | n, m \rangle \\ & \sim i \frac{e}{\hbar} (E_{n',m'} - E_{n,m}) \langle n', m' | \mathbf{A}_{\ell,\sigma}^{\text{OV}}(\theta) \cdot \mathbf{r} | n, m \rangle. \end{aligned} \quad (25)$$

This matrix element depends on the incident angle θ via (12). In this paper, we restrict our discussion to the small incident angle case, $\theta \ll 1$. After some calculations, we obtain the matrix element with θ -dependence,

$$\begin{aligned} & \langle n', m' | \mathbf{A}_{\ell, \sigma}^{\text{OV}}(\theta) \cdot \mathbf{r} | n, m \rangle \\ &= A_0 \sqrt{\frac{k_{\perp}}{4\pi}} \sum_{L=-\infty}^{\infty} e^{i\frac{\pi}{2}(L+1)} \delta_{\Delta m, \ell + \sigma + L} \\ & \times \int d\rho \rho^2 \mathfrak{R}(\rho) \mathfrak{R}_{n, m}(\rho) J_{\ell}(k_{\perp} \rho) J_L(k_{\parallel} \rho \theta). \end{aligned} \quad (26)$$

The azimuthal angular integral gives the AM conservation,

$$\Delta m = \ell + \sigma + L. \quad (27)$$

By combining this conservation, optical SAM, $\sigma = \pm 1$, and Eq. (23), it gives the modified AM selection rules,

$$\ell + L = 0, \sigma = 1, \text{ or } \ell + L = 2, \sigma = -1, \quad (28)$$

which is different from the vertically irradiated case (2). As L can be any integer number, the initial optical OAM ℓ can also be allowed to be an integer number. In other words, it is allowed that the 2DEG absorbs the OV beam with any integer OAM ℓ in oblique incidence. Putting $\theta = 0$ in (12), only the $L = 0$ term survives and the result of the vertical incidence is reproduced.

The summation over L leads to

$$\langle n', m' | \mathbf{A}_{\ell, \sigma}^{\text{OV}}(\theta) \cdot \mathbf{r} | n, m \rangle = e^{i\frac{\pi}{2}(\Delta m - \ell - \sigma + 1)} A_0 \sqrt{\frac{k_{\perp}}{4\pi}} D_{n, m, \ell}^{n', m'}(\theta), \quad (29)$$

where we denoted the radial integral in the above expression as

$$D_{n, m, \ell, \sigma}^{n', m'}(\theta) = \int d\rho \rho^2 \mathfrak{R}_{n', m'}(\rho) \mathfrak{R}_{n, m}(\rho) J_{\ell}(k_{\perp} \rho) J_{\Delta m - \ell - \sigma}(k_{\parallel} \rho \theta). \quad (30)$$

As we obtained the expressions of matrix elements, $\langle n, m | j_i | n', m' \rangle$, and $\langle n', m' | \mathbf{A}_{\ell, \sigma}^{\text{OV}}(\theta) \cdot \mathbf{j} | n, m \rangle$, we now turn to the photocurrent using the Kubo formula (17). We now concentrate our discussion on zero temperature and the filling factor is set to $\nu = 1$. Then, by (24), the left-circularly polarized current is not induced and the right one just arises in transitions from $N = 0$ to $N = 1$. The θ -dependent OV-induced photocurrent then reduces to

$$\delta j_{\ell, \sigma}^+(\theta, \omega, B) = -e^{i\frac{\pi}{2}(2-\ell-\sigma)} \frac{F_{\sigma}^{\ell}(\theta, B)}{\hbar\omega - \hbar\omega_c + i\delta}, \quad (31)$$

and the factors $F_\sigma^\ell(\theta, B)$ are given by

$$F_\sigma^\ell(\theta, B) = A_1 C_{0,0}^{0,1} D_{0,0,\ell}^{0,1}(\theta) + A_1 \sum_{m < 0}^{-m_{\max}} C_{0,m}^{1,m+1} D_{0,m,\ell,\sigma}^{1,m+1}(\theta), \quad (32)$$

with $A_1 = A_0 e^2 \omega_c^2 \sqrt{k_\perp / 2\pi} / V$. In the summation over m , only the term corresponding to the edge state survives and the other terms corresponding to the bulk states cancel each other. That is, the induced photocurrent localizes on the system edge R .

To see the net contribution of $\delta j_{\ell,\sigma}^+(\theta, \omega, B)$, we evaluate the energy denominator. When we take a clean limit $\delta \rightarrow 0$, the energy denominator is decomposed into two terms as

$$\frac{1}{\hbar\omega - \hbar\omega_c + i\delta} \rightarrow \mathcal{P} \frac{1}{\hbar\omega - \hbar\omega_c} - i\delta(\hbar\omega - \hbar\omega_c), \quad (33)$$

where \mathcal{P} indicates Cauchy principal value. We assume this principal value can be neglected around $\omega \sim \omega_c$. Then $\delta(\hbar\omega - \hbar\omega_c)$ term gives the energy conservation and a net contribution to the induced photocurrent. As the cyclotron frequency ω_c depends on the magnetic field B , the optical frequency ω also is linked to the magnetic field B via $\delta(\hbar\omega - \hbar\omega_c)$. Therefore, to observe the B dependence of $\delta j_{\ell,\sigma}^+(\theta, \omega_c, B)$, it is needed the change of the optical frequency ω or the magnitude of the wavenumber k to keep $k = \omega_c / c$.

By incorporating magnetic field dependence and using $\alpha \ll 1$ (paraxial approximation), we approximately obtain the factor $F_\sigma^\ell(\theta, B)$ for the OV beam as

$$F_\sigma^\ell(\theta, B) = F_0 \left(\frac{1 + \alpha^2}{\alpha^2} \frac{\Phi_0^2}{\lambda_e^2 B^2 R^2} \left[1 + \frac{\Phi_0}{2\pi B R^2} \right] e \right)^{\pi R^2 B / \Phi_0} \times \int dx x^{2m_{\max}+3} \exp\left(-\frac{x^2}{2k_\perp l_B}\right) J_\ell(x) J_{1-\ell-\sigma}\left(\frac{x}{\alpha} \theta\right), \quad (34)$$

where $F_0 = A_0 e^2 c^2 / V \sqrt{4\pi \lambda_e e}$, $\Phi_0 (= 2\pi \hbar / e)$ is the flux quantum, $\lambda_e (= 2\pi \hbar / m_e c)$ is the electron Compton wavelength, and $\alpha (= k_\perp / k_\parallel)$ is the ratio of paraxial approximation. Here, $x (= k_\perp \rho)$ is a dimensionless variable.

Next, we grasp the overall profile of these qualitative behaviors through the integral in Eq. (34). We decompose the integrand into

$$g(x) = x^{2m_{\max}+3} \exp\left(-\frac{x^2}{2k_\perp^2 l_B^2}\right) \quad (35)$$

and the Bessel functions,

$$h(x, \theta) = J_\ell(x) J_{1-\ell-\sigma}\left(\frac{x\theta}{\alpha}\right). \quad (36)$$

We note that $g(x)$ has its extrema at

$$x^* = \sqrt{2m_{\max} + 3k_{\perp}l_B} \simeq 587\alpha RB, \quad (37)$$

corresponds to the system edge R . Using the values $\alpha = 0.1$, $R = 10^{-2}$ m, $m_e = 9.11 \times 10^{-31}$ kg, and $c = 3.00 \times 10^8$ m/s, we have $x^* \simeq 0.587B$ with B being measured in Tesla. On the other hand, the Bessel functions factor $h(x, \theta)$ describes the interference between the initial CPBOV beam profile $J_{\ell}(x)$ and $J_{1-\ell-\sigma}(x\theta/\alpha)$. Because of the positive roots of the Bessel functions, $J_{\ell}(x) = 0$ and $J_{1-\ell-\sigma}(x\theta/\alpha) = 0$, $h(x, \theta)$ manifests zero lines in $x\theta$ -plane and demonstrate oscillating behavior. Consequently, $g(x)$ and $h(x, \theta)$ significantly interfere with each other and behave oscillation. Thus when the zeros of $J_{\ell}(x) = 0$ or $J_{1-\ell-\sigma}(x\theta/\alpha) = 0$, overlaps the peak of $g(x)$, namely x^* , $F_{\sigma}^{\ell}(\theta, B)$ is disappeared. The physical meaning of this is that the OV-induced photocurrents are disappeared when the dark rings constituted through the zeros of $J_{\ell}(k_{\perp}\rho) = 0$ and $J_{1-\ell-\sigma}(k_{\parallel}\rho\theta) = 0$ overlap the system edge R .

Here, to elucidate the salient feature of OV, it may be useful to consider the case of a purely plane wave. To see this, we give the expression of the induced photocurrent by absorption of the circularly polarized plane wave (CPPW). The vector potential of the CPPW traveling along the Z -axis is given by

$$\mathbf{A}_{\sigma}^{\text{PW}}(\mathbf{r}|\theta) = iA_0^{\text{PW}}\varepsilon_{\sigma}e^{ik_{\parallel}Z}, \quad (38)$$

where A_0^{PW} is a real constant and ε_{σ} is the circular polarization in the beam frame (4). As given in Appendix B, the PW-induced photocurrent for $\theta \ll 1$ reads

$$\delta j_{+}^{\text{PW}(\sigma)}(\omega) = -i\sigma \frac{F_{\sigma}^{\text{PW}}(\theta, B)}{\hbar\omega - \hbar\omega_c + i\delta}, \quad (39)$$

where the factor $F_{\sigma}^{\text{PW}}(\theta, B)$ is given by

$$F_{\sigma}^{\text{PW}}(\theta, B) = F_0^{\text{PW}}B^{5/2} \left(\frac{e}{R^2} \left[1 + \frac{\Phi_0}{2\pi R^2 B} \right] \right)^{\frac{\pi R^2}{\Phi_0} B} \times \int d\rho \rho^{2m_{\max}+3} \exp\left(-\frac{\rho^2}{2l_B^2}\right) J_{1-\sigma}(k_{\parallel}\rho\theta), \quad (40)$$

with $F_0^{\text{PW}} = A_0^{\text{PW}}e^2c^2\lambda_e^2/V\sqrt{2\Phi_0^5}$. Each helicity wave can induce photocurrents. In other words, that the AM selection rule for CPPW absorption is $\sigma = \pm 1$. Unlike $J_{\ell}(k_{\perp}\rho)J_{1-\ell-\sigma}(k_{\parallel}\rho\theta)$ in $F_{\sigma}^{\ell}(\theta, B)$, $J_{1-\sigma}(k_{\parallel}\rho\theta)$ appears in $F_{\sigma}^{\text{PW}}(\theta, B)$. The disappearance of PW-induced photocurrent arises from an overlap of only the positive roots of $J_{1-\sigma}(k_{\parallel}\rho\theta) = 0$. Also, when

$\theta = 0$, it gives $F_{-1}^{\text{PW}}(\theta, B) = 0$, and $F_1^{\text{PW}}(\theta, B) \neq 0$. Thus, when the vertical incidence, only the CPPW with positive helicity, $\sigma = 1$, induces the photocurrent. As the CPPW carries no OAM, this corresponds to one of the OV-absorption selection rules, $\ell = 0, \sigma = 1$.

IV. NUMERICAL RESULTS

In this section, we demonstrate the numerical results of the incident angle θ and magnetic field B dependence of $\delta j_{\ell, \sigma}^+(\theta, \omega, B)$. Figure 2 and 3 show the magnetic field B and incident angle θ dependencies of $F_{\sigma}^{\ell}(\theta, B)$ for $\ell = 0, \pm 1, \pm 2$ with each helicity when we choose the parameters as $\alpha = 0.1$, $R = 10^{-2}$ m, $m_e = 9.11 \times 10^{-31}$ kg, and $c = 3.00 \times 10^8$ m/s. Also, we give the results of the plane wave case, $F_{\sigma}^{\text{PW}}(\theta, B)$, in these figures. We here introduce the characteristic magnetic field strength, $B^* \equiv \Phi_0 / \alpha \lambda_e R$, which corresponds to $k_{\perp} R \sim 1$. Note that the wavelengths (wavenumbers) are tuned with the change of the applied magnetic field B to induce the photocurrent via energy conservation.

It is notable that the absorption amplitudes $|F_{\sigma}^{\ell}(\theta, B)|$ oscillate and evolve with increasing the magnetic field strength B . The origin of the oscillating behavior in change B is as follows. When B changes, the dark ring radius of the OV intensity which is determined by the positive root of $J_{\ell}(k_{\perp} \rho) = 0$ changes with the transverse wavenumber $k_{\perp} (= 587\alpha B)$ with fixed α . When the dark ring overlaps the system edge R where the photocurrent is localizing, the induced photocurrent is disappeared. Also, the origin of this evolutionary behavior in change B is as follows. When B increases, it narrows the width of the electron wavefunction which is linked by the magnetic length l_B . Then the number of electrons in the LLL becomes increasing because the chemical potential is kept between the LLL ($N = 0$) and the second LL ($N = 1$). Thus the number of electrons contributing to the induced photocurrent increases in increasing B . Further, it is noted that the absorption amplitudes oscillate in the change of the incident angle θ . The reason is why the dark rings of obliquely irradiated OV intensity depend on the positive roots of $J_{1-\ell-\sigma}(k_{\parallel} \rho \theta) = 0$ as well. When the dark ring in the change θ overlaps the system edge R , the induced photocurrent is disappeared in analogy with the case of change B .

Consequently, there exist the lattice-shaped disappearance pattern due to the interference between the positive roots of Bessel function, $J_{\ell}(k_{\perp} \rho) = 0$, and $J_{1-\ell-\sigma}(k_{\parallel} \rho \theta) = 0$. In particular, the vertical incidence, $\theta = 0$, gives no induced photocurrent except for $\ell = 0$,

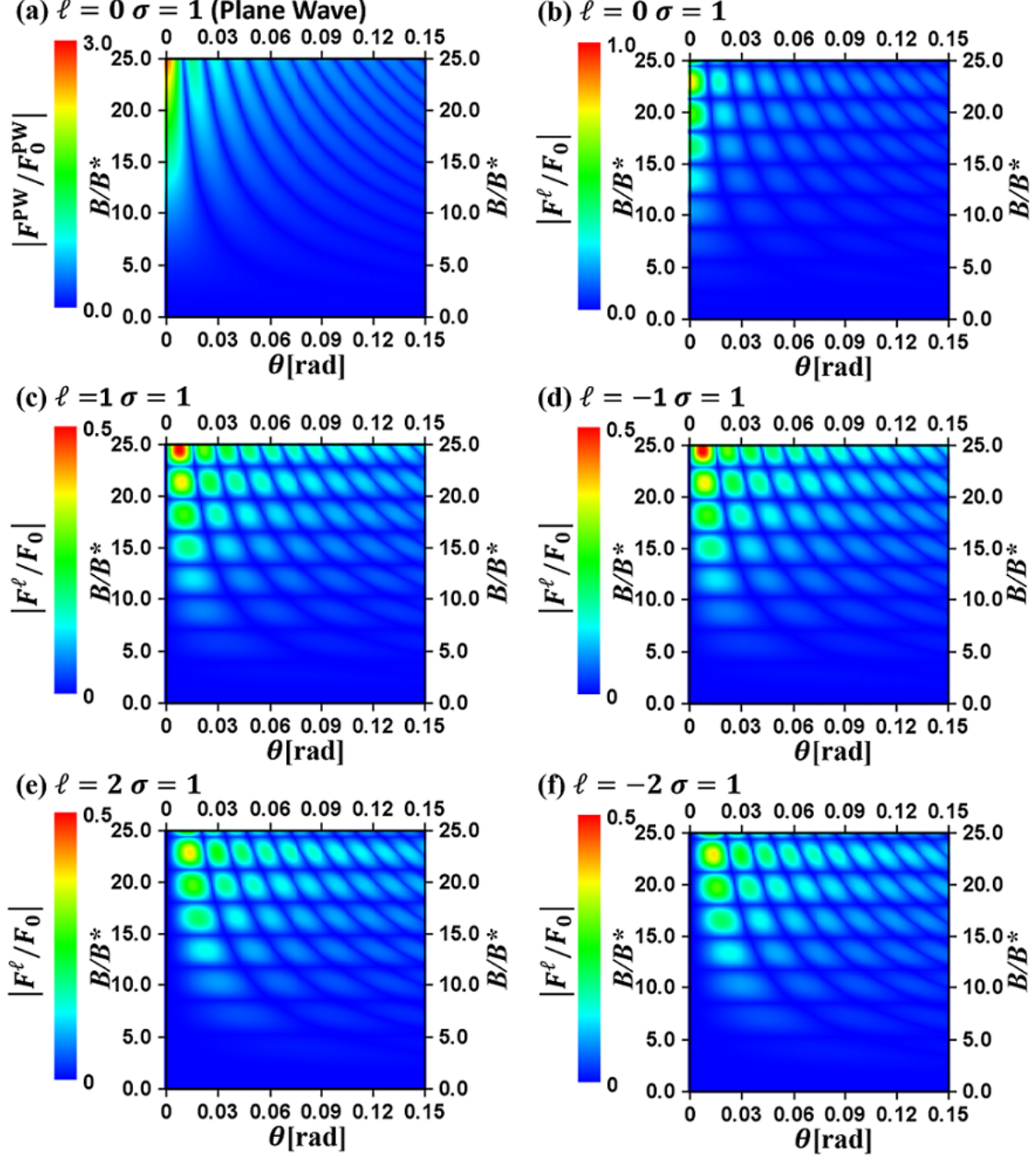


FIG. 2. The contour plots of the θ and B dependence of intensity F_σ^ℓ and F_σ^{PW} for positive helicity waves when the chemical potential is kept between the LLL and second LL. (a) plane wave ($\ell = 0$), (b) vortex wave with $\ell = 0$, (c) $\ell = 1$, (d) $\ell = -1$, (e) $\ell = 2$, (f) $\ell = -2$. Parameters are $R = 10^{-2}$ m in system size and $\alpha = 0.1$ with $\alpha = k_\perp/k_\parallel$. The wavenumber has B dependence as $k = 5.87 \times 10^2 B$ [m^{-1}]. The vertical axes are scaled by $B^* = \Phi_0/\alpha\lambda_e R = 1.70 \times 10^{-3}/\alpha R$ [T].

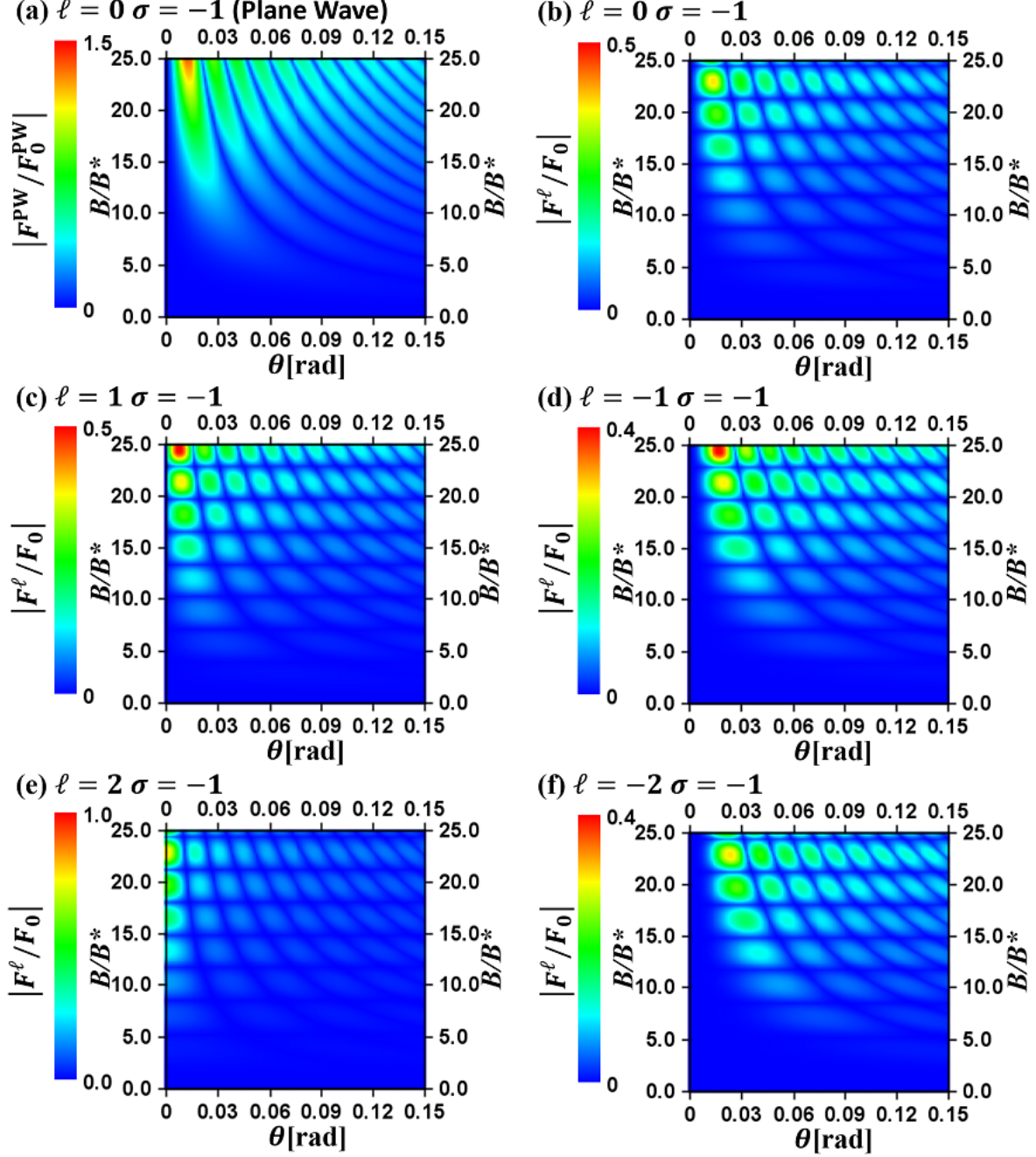


FIG. 3. The contour plots of the θ and B dependence of intensity F_σ^ℓ and F_σ^{PW} for negative helicity waves when the chemical potential is kept between the LLL and second LL. (a) plane wave ($\ell = 0$), (b) vortex wave with $\ell = 0$, (c) $\ell = 1$, (d) $\ell = -1$, (e) $\ell = 2$, (f) $\ell = -2$. Parameters are $R = 10^{-2}$ m in system size and $\alpha = 0.1$ with $\alpha = k_\perp/k_\parallel$. The wavenumber has B dependence as $k = 5.87 \times 10^2 B$ [m^{-1}]. The vertical axes are scaled by $B^* = \Phi_0/\alpha\lambda_e R = 1.70 \times 10^{-3}/\alpha R$ [T].

$\sigma = 1$, and $\ell = 2$, $\sigma = -1$. These results are equivalent to the results shown in our previous paper.[30, 42]

V. CONCLUSIONS AND REMARKS

We have investigated the modification of selection rules in induced photocurrents by coupling the Landau-quantized system with obliquely irradiated OV beams. As discussed in our previous paper, the Landau-quantized system is suitable for causing interaction with OVs. The reasons are as follows: It is known that the optical OAM can not be transferred to the internal motion but the center-of-mass motion in an electric dipole transition.[29] To transfer the optical OAM to the electron center-of-mass motion through the electric dipole transition, it is needed to match the OV spatial structure with the electron system geometry. In other words, if the intensity profile of OV beams has an axially symmetrical structure around the optical axis, the electron system geometry should have axial symmetry. Therefore, we considered that the best choice is a 2DEG confined on a circular disk geometry. Furthermore, to discuss the absorption of the orbital and spin AM, a paraxial approximation of OV beams is important. Absorptions of optical AM to the photocurrent are confined to optical TAM of one, $J = 1$. Thus, in the vertical incidence, the combinations of the optical OAM and SAM are locked as only Eq. (2) because of the conservation of OAM.[30] However, it is inevitable to consider the case of oblique incidence from the experimental viewpoints. Since the obliquely irradiated (angular deflected) beam consists of a superposition of the various OAM, $\ell + L$, with initial optical OAM ℓ and arbitrary orbit number L .[31] Thus, in this paper, it was explicitly shown that the partial wave carrying the OAM, $\ell + L$, is absorbed by 2DEG and it modifies AM selection rule, $\ell + \sigma + L = 1$. In other words, absorptions of any integer initial optical OAM ℓ are allowed in the oblique incidence.

We also showed oscillating behaviors of the OV-induced photocurrent in a change of the incident angle θ and the magnetic field B . The oscillating behavior has its origin in the interferences between the profile of light intensity and that of the current localized on the system edge. Especially, as the obliquely irradiated OV beam seems a superposition of partial waves with the θ -dependent Bessel function type amplitude,[31] the OV-induced current also has θ -dependent oscillating behavior. On the other hand, it is noted that as the obliquely irradiated purely plane wave is also described by a superposition of partial wave with the

θ -dependent Bessel function type amplitude, the θ -dependent oscillating behavior is yielded even in the case of the purely plane wave. Nevertheless, as the OV has a characteristic intensity profile (Bessel-mode, LG-mode, and elsewhere), the oscillating behavior different from the case of the purely plane wave is yielded.

In our numerical results, the bare electron mass was used. However, the effective (cyclotron) mass m_e^* should be used for actual materials. As the cyclotron frequency, $\omega_c = eB/m_e^*$, is then changed, the wavenumber is also changed via the energy conservation in transitions from the LLL to the second LL. This affects the radius of the bright and dark rings. For example, for the widely accepted value, $m_e^* = 0.067m_e$, for GaAs, the wavenumber of the OV beam is evaluated as $k/0.067$. Then the bright and dark rings become 0.067 times larger in radius. Therefore, it is needed to pay attention to suitable 2DEG system size R to match with the OV spatial structure in experiments.

ACKNOWLEDGMENTS

The authors thank Dr. S. Hashiyada, I. Proskurin, Professors Y. Yamada, K. Oto, and Y. Togawa for fruitful discussions. This work was supported by JSPS KAKENHI Grant (25220803, 17H02923), and the JSPS Bilateral (Japan-Russia) Joint Research Projects.

Appendix A: Long-Wavelength Approximation in Light-Electron Coupling Hamiltonian

In this Appendix, we discuss the validity of the long-wavelength approximation in Eq. (25). We first show the commutation relation, $[H_0, \mathbf{A}^{\text{OV}}]$, with non-perturbative Hamiltonian, $H_0 = \frac{1}{2m_e^*} (-i\hbar\nabla + e\mathbf{A}^{\text{ext}})^2$. Note that a vector potential of OV is described by $\mathbf{A}^{\text{OV}} = \varepsilon_\sigma f(k_\perp \rho) e^{i\ell\phi + ik_\parallel z}$ with $\nabla \cdot \mathbf{A}^{\text{OV}} = 0$, and $\text{grad} [f(k_\perp \rho) e^{i\ell\phi + ik_\parallel z}] \sim \mathbf{k} f(k_\perp \rho) e^{i\ell\phi + ik_\parallel z}$. After some calculations, we obtain

$$H_0 \mathbf{A}^{\text{OV}} \approx \mathbf{A}^{\text{OV}} H_0 + \mathbf{A}^{\text{OV}} \left\{ \frac{\hbar^2 k^2}{2m_e^*} - \left(\frac{\hbar \mathbf{k}}{m_e^*} \right) \cdot (-i\hbar\nabla) + \frac{e}{m_e^*} (\mathbf{A}^{\text{ext}} \cdot \hbar \mathbf{k}) \right\}. \quad (\text{A1})$$

Therefore, the commutation relation is written by

$$[H_0, \mathbf{A}^{\text{OV}}] = \mathbf{A}^{\text{OV}} \left\{ \frac{\hbar^2 k^2}{2m_e^*} - \left(\frac{\hbar \mathbf{k}}{m_e^*} \right) \cdot (-i\hbar\nabla) + \frac{e}{m_e^*} (\mathbf{A}^{\text{ext}} \cdot \hbar \mathbf{k}) \right\}. \quad (\text{A2})$$

Next, we evaluate the matrix element of the light-electron coupling, $\langle n', m' | \mathbf{A}^{\text{OV}} \cdot \mathbf{j} | n, m \rangle$, with a photocurrent operator, $\mathbf{j} = \frac{e}{m_e^*} (\mathbf{p} + e\mathbf{A}^{\text{ext}})$. Noting that the photocurrent operator satisfies

$$\mathbf{j} = \mathbf{p} + e\mathbf{A}^{\text{ext}} = \frac{im_e^*}{\hbar} [H_0, \mathbf{r}] \quad (\text{A3})$$

by using the commutation relation (A2), we obtain

$$\begin{aligned} \langle n', m' | \mathbf{A}^{\text{OV}} \cdot \mathbf{j} | n, m \rangle &= \frac{e}{m_e} \langle n', m' | \mathbf{A}^{\text{OV}} \cdot \frac{im_e}{\hbar} [H_0, \mathbf{r}] | n, m \rangle \\ &= \frac{ie}{\hbar} (E_{n', m'} - E_{n, m}) \langle n', m' | \mathbf{A}^{\text{OV}} \cdot \mathbf{r} | n, m \rangle \\ &\quad - \frac{ie \hbar^2 k^2}{\hbar 2m_e} \langle n', m' | \mathbf{A}^{\text{OV}} \cdot \mathbf{r} | n, m \rangle \\ &\quad - \frac{ie \hbar e}{\hbar m_e} \langle n', m' | (\mathbf{A}^{\text{ext}} \cdot \mathbf{k})(\mathbf{A}^{\text{OV}} \cdot \mathbf{r}) | n, m \rangle \\ &\quad - \frac{e \hbar^2}{\hbar 2m_e} \langle n', m' | \mathbf{A}^{\text{OV}} \cdot \mathbf{k} | n, m \rangle \\ &\quad - \frac{e \hbar^2}{\hbar 2m_e} \langle n', m' | (\mathbf{A}^{\text{OV}} \cdot \mathbf{r}) \mathbf{k} \cdot \text{grad} | n, m \rangle. \end{aligned} \quad (\text{A4})$$

In the long-wavelength approximation, the second term is the second order in k . It is 10^9 times weaker than the first term in $B = 10$ T and can be dropped. Furthermore, as the third, fourth, and fifth terms in (A4) have the first order in k , which is 10^5 times weaker than the first term in $B = 10$ T. Then these terms can also be ignored by the comparison with the first term. As a consequence, the first term only survives in the matrix element of the light-electron coupling,

$$\langle n', m' | \mathbf{A}^{\text{OV}} \cdot \mathbf{j} | n, m \rangle \sim \frac{ie}{\hbar} (E_{n', m'} - E_{n, m}) \langle n', m' | \mathbf{A}^{\text{OV}} \cdot \mathbf{r} | n, m \rangle. \quad (\text{A5})$$

which is Eq. (25).

Appendix B: Induced Current by Circularly Polarized Plane Wave

To compare the OV-induced photocurrent with PW-induced one, we derive (39) and (40). In the case of the circularly polarized plane wave (38), its vector potential in the Laboratory frame is given by

$$\begin{aligned} \mathbf{A}_\sigma^{\text{PW}}(\mathbf{r}|\theta) &= \frac{A_0^{\text{PW}}}{\sqrt{2}} (\mathbf{e}_x \cos \theta + i\sigma \mathbf{e}_y - \mathbf{e}_z \sin \theta) \\ &\quad \times \sum_{L=-\infty}^{\infty} J_L(k_{\parallel} \rho \sin \theta) e^{i\frac{\pi}{2}(L+1)} e^{iL\phi} e^{ik_{\parallel} z \cos \theta}. \end{aligned} \quad (\text{B1})$$

Then the matrix element of the light-electron coupling is given by

$$\begin{aligned}
& \langle n', m' | \mathbf{A}_\sigma^{\text{PW}}(\theta) \cdot \mathbf{r} | n, m \rangle \\
& \sim \frac{A_0^{\text{PW}}}{\sqrt{2}} \sum_{L=-\infty}^{\infty} e^{\frac{\pi}{2}(L+1)} \int d\rho \rho^2 R_{n', m'}(\rho) R_{n, m}(\rho) J_L(k_{\parallel} \rho \sin \theta) \\
& \times \left\{ \cos^2 \frac{\theta}{2} \delta_{\Delta m, L+\sigma} - \sin^2 \frac{\theta}{2} \delta_{\Delta m, L-\sigma} \right\}. \tag{B2}
\end{aligned}$$

When we assume $\theta \ll 1$, we obtain

$$\begin{aligned}
& \langle n', m' | \mathbf{A}_\sigma^{\text{PW}}(\theta) \cdot \mathbf{r} | n, m \rangle \\
& \sim \frac{A_0^{\text{PW}}}{\sqrt{2}} \sum_{L=-\infty}^{\infty} e^{\frac{\pi}{2}(L+1)} \int d\rho \rho^2 R_{n', m'}(\rho) R_{n, m}(\rho) J_L(k_{\parallel} \rho \theta) \delta_{\Delta m, L+\sigma}, \tag{B3}
\end{aligned}$$

where the second term was dropped because of $O(\theta^2)$. After the summation over L , the matrix element reduces to

$$\begin{aligned}
& \langle n' m' | \mathbf{A}_\sigma^{\text{PW}}(\theta) \cdot \mathbf{r} | n, m \rangle \\
& \sim \frac{A_0^{\text{PW}}}{\sqrt{2}} e^{\frac{\pi}{2}(\Delta m - \sigma + 1)} \int d\rho \rho^2 R_{n', m'}(\rho) R_{n, m}(\rho) J_{\Delta m - \sigma}(k_{\parallel} \rho \theta). \tag{B4}
\end{aligned}$$

When we proceed with the same procedure for the OV case to obtain the induced photocurrent, it gives

$$\delta j_\sigma^{+\text{PW}}(\theta, \omega, B) = -i\sigma \frac{F_\sigma^{\text{PW}}(B, \theta)}{\hbar\omega - \hbar\omega_c + i\delta}, \tag{B5}$$

where we defined the factor as

$$\begin{aligned}
F_\sigma^{\text{PW}}(B, \theta) &= F_0^{\text{PW}} B^{5/2} \left(\frac{e}{R^2} \left[1 + \frac{\Phi_0}{2\pi R^2 B} \right] \right)^{\frac{\pi R^2}{\Phi_0} B} \\
&\times \int_0^R d\rho \rho^{2m_{\text{max}}+3} \exp\left(-\frac{\rho^2}{2l_B^2}\right) J_{-\sigma+1}(k_{\parallel} \rho \theta), \tag{B6}
\end{aligned}$$

with $F_0^{\text{PW}} = A_0^{\text{PW}} e^2 c^2 \lambda_e^2 / V \sqrt{2\Phi_0^5 e}$. These are Eqs. (39) and (40).

-
- [1] J. H. Poynting, Proc. R. Soc. Lond. Ser. A **82**, 560 (1909).
 - [2] R. A. Beth, Phys. Rev. **50**, 115 (1936).
 - [3] L. Allen, M. W. Beijersbergen, R. J. C. Spreeuw, and J. P. Woerdman, Phys. Rev. A **45**, 8185 (1992).

- [4] C. Tamm and C. O. Weiss, *J. Opt. Soc. Am. B* **7**, 1034 (1990).
- [5] M. Harris, C. A. Hill, J. M. Vaughan, *Opt. Commun.* **106**, 161 (1994).
- [6] M. W. Beijersbergen, L. Allen, H. van der Veen, J. P. Woerdman, *Opt. Commun.* **96**, 123 (1993).
- [7] M. W. Beijersbergen, R. P. C. Coerwinkel, M. Kristensen, and J. P. Woerdman, *Opt. Commun.* **112**, 321 (1994).
- [8] N. R. Heckenberg, R. McDuff, C. P. Smith, and A. G. White, *Opt. Lett.* **17**, 221 (1992).
- [9] S. A. Kennedy, M. J. Szabo, H. Teslow, J. Z. Porterfield, and E. R. I. Abraham, *Phys. Rev. A* **66**, 043801 (2002).
- [10] K. Nakagawa, K. Yamane, R. Morita, and Y. Toda, *Appl. Phys. Express* **13**, 042001 (2020).
- [11] U. D. Jentschura and V. G. Serbo, *Phys. Rev. Lett.* **106**, 013001, (2011).
- [12] J. Durnin, *J. Opt. Soc. Am. B* **4**, 651 (1987).
- [13] D. McGloin and K. Dholakia, *Contemporary Physics*, **46**, 15 (2005).
- [14] J. Durnin, J.J. Miceli, and J.H. Eberly, *Phys. Rev. Lett.* **58**, 1499 (1987).
- [15] G. Indebetouw, *J. Opt. Soc. Am. A-Opt. Image Sci. Vis.* **6**, 150 (1989).
- [16] A. Vasara, J. Turunen and A.T. Friberg, *J. Opt. Soc. Am. A-Opt. Image Sci. Vis.* **6**, 1748 (1989).
- [17] A.J. Cox and D.C. Dibble, *J. Opt. Soc. Am. A-Opt. Image Sci. Vis.* **9**, 282 (1992).
- [18] B Amos, and P Gill, *Meas. Sci. Technol.*, **6**, 248 (1995).
- [19] H. He, M. E.J. Friese, N. R. Heckenberg, and H. Rubinsztein-Dunlop, *Phys. Rev. Lett.* **75**, 826 (1995).
- [20] K. Shigematsu, K. Yamane, R. Morita, and Y. Toda, *Phys. Rev. B* **93**, 045205 (2016).
- [21] C. T. Schmiegelow, J. Schulz, H. Kaufmann, T. Ruster, U. G. Poschinger, and F. Schmidt-Kaler, *Nat. Commun.*, **7**, 12998 (2016).
- [22] J. Hamazaki, R. Morita, K. Chujo, Y. Kobayashi, S. Tanda, and T. Omatsu, *Opt. Express* **18**, 2144 (2010).
- [23] G. F. Quinteiro and P. I. Tamborenea, *Europhys. Lett.* **85**, 47001 (2009).
- [24] J. Wätzel, A. S. Moskalenko, and J. Berakdar, *Opt. Express* **20**, 27792 (2012).
- [25] K. Sakai, K. Nomura, T. Yamamoto, and K. Sasaki, *Sci. Rep.* **5**, 8431 (2015).
- [26] K. Shintani, K. Taguchi, Y. Tanaka, and Y. Kawaguchi, *Phys. Rev. B* **93**, 195415 (2016).
- [27] H. Fujita and M. Sato, *Phys. Rev. B* **95**, 054421 (2017).

- [28] T. Yokoyama, J. Phys. Soc. Jpn. **89**, 103703 (2020).
- [29] M. Babiker, C. R. Bennett, D. L. Andrews, and L.C. Dávila Romero, Phys. Rev. Lett. **89**, 143601 (2002).
- [30] H. Takahashi, I. Proskurin, and J.-i. Kishine, J. Phys. Soc. Jpn. **87**, 113703 (2018).
- [31] M. V. Vasnetsov, V. A. Pas'ko, and M. S. Soskin, New J. Phys. **7**, 46 (2005).
- [32] M. P. Lavery, G. C. Berkhout, J. Courtial, and M. J. Padgett, J. Opt. **13**, 064006 (2011).
- [33] S. J. van Enk and G. Nienhuis, Opt. Commun. **94**, 147–58 (1992).
- [34] G. Molina-Terriza, J. P. Torres, and L. Torner, Phys. Rev. Lett. **88**, 013601 (2002).
- [35] A. T. O'Neil, I. MacVicar, L. Allen, and M. J. Padgett, Phys. Rev. Lett. **88**, 053601 (2002).
- [36] O. Matula, A. G. Hayrapetyan, V. G. Serbo, A. Surzhykov, and S. Fritzsche, J. Phys. B: At. Mol. Opt. Phys. **46**, 205002 (2013).
- [37] M. Abramowitz and I. A. Stegun, *Handbook of Mathematical Functions with Formulas, Graphs, and Mathematical Tables* (Dover, 1965)
- [38] C. Cohen-Tannoudji, G. Grynberg, and J. Dupont-Roc, *Photons and Atoms: Introduction to Quantum Electrodynamics* (Wiley, 1997).
- [39] L. D. Landau and L. M. Lifshitz, *Quantum Mechanics: Non-Relativistic Theory*. 3rd ed. (Pergamon, 1991).
- [40] R. Kubo, J. Phys. Soc. Jpn. **12**, 570 (1957).
- [41] T. Ando, J. Phys. Soc. Jpn, **38** 989 (1975).
- [42] H. Takahashi, I. Proskurin, and J.-i. Kishine, arXiv:1904.03083.